JACS
JOURNAL OF THE AMERICAN CHEMICAL SOCIETY
Article
pubs.acs.org/JACS

Direct Detection of Key Reaction Intermediates in Photochemical CO_2 Reduction Sensitized by a Rhenium Bipyridine Complex

Youki Kou,[†] Yu Nabetani,[†,‡] Dai Masui,[†,§] Tetsuya Shimada,[†,‡] Shinsuke Takagi,[†,‡] Hiroshi Tachibana,[†,‡] and Haruo Inoue*[,†,‡]

[†]Department of Applied Chemistry, Graduate School of Urban Environmental Sciences, Tokyo Metropolitan University, 1-1 Minami-osawa, Hachioji, Tokyo 192-0397, Japan

[‡]Center for Artificial Photosynthesis, Tokyo Metropolitan University, 1-1 Minami-osawa, Hachioji, Tokyo 192-0397, Japan

Supporting Information

ABSTRACT: Photochemical CO_2 reduction sensitized by rhenium–bipyridyl complexes has been studied through multiple approaches during the past several decades. However, a key reaction intermediate, the CO_2-coordinated Re–bipyridyl complex, which should govern the activity of CO_2 reduction in the photocatalytic cycle, has never been detected in a direct way. In this study on photoreduction of CO_2 catalyzed by the 4,4′-dimethyl-2,2′-bipyridine (dmbpy) complex, $[Re(dmbpy)(CO)_3Cl]$ (**1**), we successfully detect the solvent-coordinated Re complex $[Re(dmbpy)(CO)_3DMF]$ (**2**) as the light-absorbing species to drive photoreduction of CO_2. The key intermediate, the CO_2-coordinated Re–bipyridyl complex, $[Re(dmbpy)(CO)_3(COOH)]$, is also successfully detected for the first time by means of cold-spray ionization spectrometry (CSI-MS). Mass spectra for a reaction mixture with isotopically labeled $^{13}CO_2$ provide clear evidence for the incorporation of CO_2 into the Re–bipyridyl complex. It is revealed that the starting chloride complex **1** was rapidly transformed into the DMF-coordinated Re complex **2** through the initial cycle of photoreduction of CO_2. The observed induction period in the time profile of the CSI-MS signals can well explain the subsequent formation of the CO_2-coordinated intermediate from the solvent-coordinated Re–bipyridyl complex. An FTIR study of the reaction mixture in dimethyl sulfoxide clearly shows the appearance of a signal at 1682 cm^{-1}, which shifts to 1647 cm^{-1} for the $^{13}CO_2$-labeled counterpart; this is assigned as the CO_2-coordinated intermediate, Re^{II}–COOH. Thus, a detailed understanding has now been obtained for the mechanism of the archetypical photochemical CO_2 reduction sensitized by a Re–bipyridyl complex.

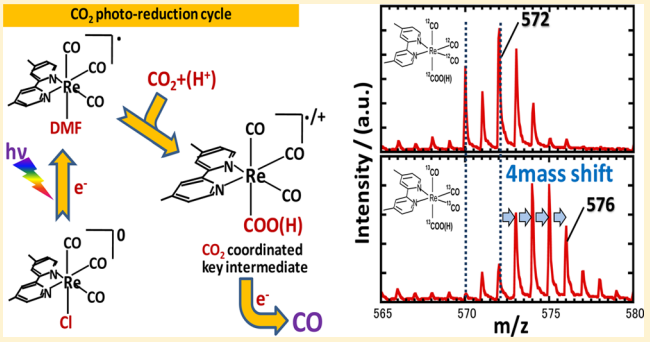

INTRODUCTION

Carbon dioxide (CO_2), well known as a greenhouse gas, which causes global warming, is also an abundant carbon resource for fuels and organic materials.[1] The development of an effective method for the fixation of atmospheric CO_2 is a global issue to be achieved for mankind from the viewpoint of realizing a sustainable society. Artificial photosynthesis, in which CO_2 is reduced with water as an electron donor, is very much anticipated to be one of the most crucial key technologies to sustain our society.[2]

Generally, it is very difficult to directly induce the one-electron reduction of CO_2 to its radical anion, $CO_2^{\bullet-}$, because the reduction potential is highly unfavorable (−2.14 V vs SCE).[1] Among various studies, including the photoelectrochemical reduction of CO_2 by *p*-type semiconductors such as *p*-GaP, *p*-CdTe, *p*-GaAs, *p*-Si, *p*-SiC, *p*-InP, etc.,[3] electrochemical reduction,[4,5] and photochemical reduction,[6] a seminal, pioneering report by Lehn et al. on the rhenium–bipyridyl complex $[Re(bpy)(CO)_3X]$,[7,8] which can efficiently induce CO_2 reduction to carbon monoxide (CO) upon UV-light irradiation, had led to intense studies on multiple aspects of the photocatalysis, e.g., synthesis, electrochemical properties, photochemical reactivity, product analysis, reaction dynamics, and so on, during the past several decades.[9−11] For example, Hori et al. reported that the reactivity of photochemical CO_2 reduction could be dramatically improved with the *fac*-$[Re(bpy)(CO)_3(P(OEt)_3)]^+$ complex, replacing the chloride ligand with a triethylphosphite (quantum yield Φ_{CO} = 38%).[10] In recent years, the efficiency of CO_2 reduction by Re–bipyridyl complexes was amazingly improved by Ishitani's group under UV light irradiation,[11] even though the electron donors are still limited to sacrificial reagents such as amines. At the present stage, how the photoreduction could be induced by visible light and how the photoreduction could be coupled with the oxidation of the water molecule should be central subjects to be resolved from the viewpoint of artificial photosynthesis. As such, the Ishitani, Inoue, and Perutz groups each reported

Received: January 14, 2014
Published: April 1, 2014

   dx.doi.org/10.1021/ja500403e | *J. Am. Chem. Soc.* 2014, 136, 6021−6030

visible-light-induced CO_2 reduction, but still with sacrificial electron donors.[12−19] Recently, we reported a visible-light-induced photoelectrochemical CO_2 reduction sensitized by a rhenium bipyridine/zinc porphyrin dyad on NiO as a non-sacrificial electron donor.[9,17] Even though photoreduction of CO_2 by the dyad provided a novel reaction mechanism through the upper excited S_2 level, it is still necessary to improve the efficiency of CO_2 reduction from a practical viewpoint. Photochemical CO_2 reduction catalyzed by metal complexes on *p*-type semiconductors has been reported.[20−23] The formation of formic acid from CO_2 and water has also been reported.[23] This system, however, was obliged to use UV light irradiation of a TiO_2 semiconductor to oxidize water.[23] The state of the art in photochemical reduction of carbon dioxide clearly requires more fundamental studies to get through various bottlenecks in order to achieve more realistic prospects for artificial photosynthesis.[1,24−28]

The Re complex has served as one of the benchmark complexes for photoreduction of CO_2, but the reaction mechanisms are not yet fully understood, despite extensive studies. Deeper insights into the reaction mechanism, and into the nature of the key factors controlling the photochemical reduction of CO_2, would be most desirable.

The mechanism of the photochemical CO_2 reduction sensitized by Re−bipyridyl complexes has been studied so far by UV−visible absorption spectroscopy,[11,29−31] electrospray ionization mass spectrometry (ESI-MS),[32,33] liquid chromatography (LC) coupled with ESI-MS (LC-ESI-MS),[34] and IR spectroscopy.[35,36] In particular, the Fujita group reported a transient FTIR study of the Re−bipyridyl complex.[35] They proposed that a CO_2-mediated dimer of Re−bipyridyl complexes could be a key intermediate for CO_2 reduction in acetonitrile (CH_3CN) or tetrahydrofuran (THF), although its reactivity was not mentioned in detail.[27,35] Regrettably, CH_3CN and THF are both rather exceptional solvents, in which photoreduction of CO_2 has only a poor reactivity, compared with a frequently used solvent such as dimethylformamide (DMF). The formation of a formate Re complex as a minor side reaction product was studied by NMR[8] in the photochemical reduction and by IR spectroscopy in the electrochemical reduction.[37] A one-electron-reduced species of the Re complex was also studied by electron paramagnetic resonance (EPR) spectroscopy.[38,39] On the basis of the previous studies, a generally proposed photochemical CO_2 reduction cycle of $[Re(bpy)(CO)_3Cl]$ is summarized in Scheme 1. In a solution of $[Re(bpy)(CO)_3Cl]$ with triethylamine as a sacrificial electron donor, a one-electron-reduced species is formed through the triplet metal-to-ligand charge-transfer (^{3}MLCT) state upon photoexcitation.[29−31] After elimination of the Cl^- ion, CO_2 may be reduced to CO by the activated Re−bipyridyl complex. The details of the reaction mechanism have not yet been clarified, since the direct detection of the intermediate, which could rationalize the observed photoreduction of CO_2, has not yet been achieved.

Against this background, herein we report the direct detection of the key reaction intermediate in the photochemical CO_2 reduction with the 4,4′-dimethyl-2,2′-bipyridyl (dmbpy) complex, $[Re(dmbpy)(CO)_3Cl]$ (**1**), by a cold spray ionization mass spectrometry (CSI-MS) method and FTIR studies. CSI-MS enables an extremely soft ionization[40,41] and is suitable for detecting rather weakly bound association complexes in solution, which can easily decompose in the ionization chamber with ordinary ESI-MS under more severe ionization conditions.

Scheme 1. Proposed Photochemical CO_2 Reduction Cycle Sensitized by a Rhenium−Bipyridyl Complex

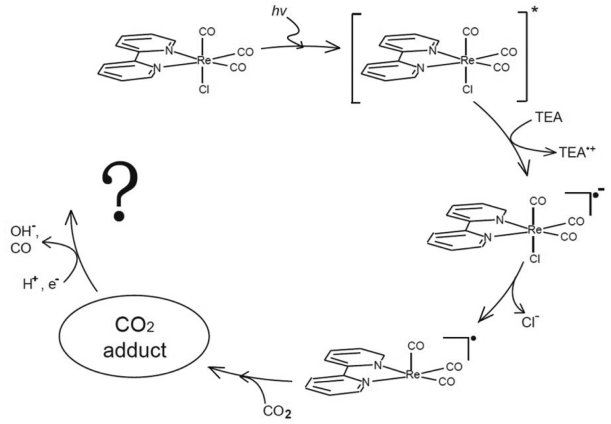

The key intermediate of the Re−bipyridyl complex, after reaction with CO_2 in the reaction pathway, is successfully observed by positive-ion mode CSI-MS for the first time. An experiment involving the photochemical reaction with isotopically labeled $^{13}CO_2$ also provides concrete evidence for CO_2 coordination to the Re−bipyridyl complex in the reaction pathway. Furthermore, the time-dependent profiles of the signals are well correlated with the time profile of CO formation in the photochemical CO_2 reduction. An FTIR study on steady-state light irradiation clearly indicates that the CO_2-coordinated species is Re^{II}−COOH. Thus, the mechanism of photochemical CO_2 reduction sensitized by the Re−bipyridyl complex is explained in detail.

EXPERIMENTAL SECTION

Materials. $[Re(dmbpy)(CO)_3Cl]$ (**1**) was synthesized according to the literature.[42] *N*,*N*′-Dimethylformamide (DMF, Kanto Chemical Co., Inc.) was used as a solvent after dehydration with 4 Å molecular sieves (Kanto Chemical Co., Inc.) and distillation under reduced pressure. Triethylamine (TEA, Kanto Chemical Co., Inc.) was used as a sacrificial electron donor in the photochemical reaction after dehydration with potassium hydroxide (Kanto Chemical Co., Inc.) and distillation. Highly pure CO_2 (>99.995%, Taiyo Nippon Sanso Co., Inc.) was used, and isotopically labeled $^{13}CO_2$ (chemical purity specification >99.9%) was purchased from Cambridge Isotope Laboratories Inc. and used as received.

Photocatalytic Reaction. **1** (0.94 mg, 0.4 mM) was dissolved in 4.8 mL of DMF/TEA solvent (v/v = 5/1). CO_2 bubbling was carried out for 30 min before photoirradiation. The samples in an L-type quartz cell (optical length, 4 cm, Eikosha) were irradiated with monochromatic light (365 nm) through an interference filter (KL-365) and an IR cut-off filter (KG1(EDMOND)) from a 500-W xenon arc lamp (USHIO 500-DKO). The amount of reduced product, CO, was measured by gas chromatography with a thermal conductivity detector (GC-TCD, Shimadzu GC-2014, equipped with a 5 Å molecular sieves column).

CSI-MS Experiment. CSI-MS was performed on a JMS-T100CS instrument (JEOL) for analyzing the reaction intermediates. Typical measurement conditions were as follows: needle voltage, 0 kV; orifice 1 voltage, −90 V; orifice 2 voltage, −10 V; sample flow rate, 0.1 mL/min; spray temperature, −10 °C; ion source temperature, −5 °C. Each sample, upon photoirradiation (0, 30, 180, 270, and 1000 min), was independently prepared and directly injected into the ion chamber of the CSI mass spectrometer with a syringe.

FTIR Experiment. The FTIR spectrum of the reaction mixture in dimethyl sulfoxide (DMSO) under steady-state light irradiation was measured by IR monitoring in rapid scan mode on a Shimadzu IRTracer-100.

dx.doi.org/10.1021/ja500403e | J. Am. Chem. Soc. 2014, 136, 6021−6030

RESULTS AND DISCUSSION

Time Profile of CO Evolution upon UV Light Irradiation. Figure 1 shows a time profile of CO evolution

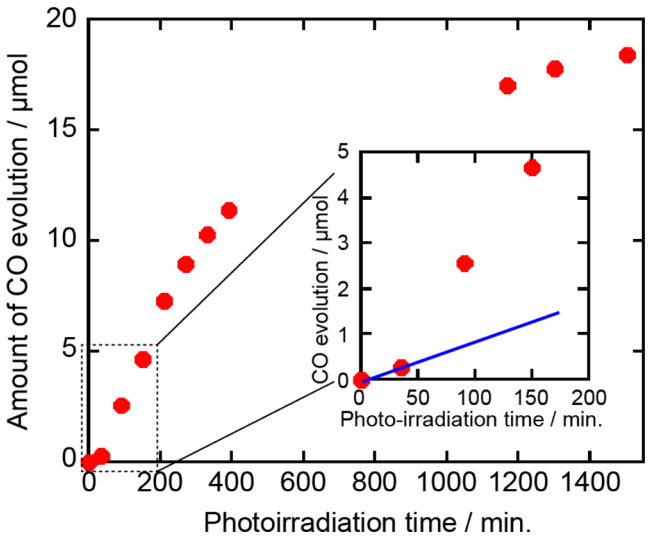

Figure 1. CO evolution catalyzed by [Re(dmbpy)(CO)$_3$Cl] (**1**) in DMF solvent with TEA (v/v = 5/1) as a sacrificial electron donor upon UV light irradiation (λ = 365 nm, 2 mW).

catalyzed by [Re(dmbpy)(CO)$_3$Cl] (**1**) in DMF including TEA as a sacrificial electron donor upon UV light irradiation (λ = 365 nm). The CO evolution increased moderately in the initial period, suggestive of an induction period within the initial 30 min. In the case of photoinduced CO_2 reduction catalyzed by [Re(dmbpy)(CO)$_3$(NCS)], a similar induction period was also reported to be caused by the dissociation of the NCS ligand in the early stage of the reaction.[43] After 30 min, the CO evolution was strongly accelerated, with a Φ_{CO} value of 10.5%, and then it decreased gradually after 500 min, probably owing to transformation or decomposition of the Re complex under the prolonged photoirradiation.

CSI-MS Measurement of the Reaction Mixture during Photoirradiation. To detect reaction intermediates, the reaction mixtures at appropriate times (0, 30, 180, 270, and 1000 min) covering the induction period, the most reactive stage, and the saturated stage were analyzed by positive-ion mode CSI-MS. The spectra obtained by CSI-MS measurement are shown in Figure 2. In the reaction mixture before the photoirradiation (Figure 2 (i), 0 min), the starting Re complex **1** exhibited mass peaks at m/z = 592, assigned as [Re(dmbpy)(CO)$_3$Cl + TEA + H$^+$], and at m/z = 608, assigned as [Re(dmbpy)(CO)$_3$Cl + CO_2 + DMF + H$^+$]. The mass patterns were well simulated by characteristic inclusion of one chlorine atom in each case (Figure S1). In contrast, ordinary positive-ion mode ESI-MS did not exhibit a peak from the starting Re complex in solution, even before the photoirradiation (Figure S2). Only a mass peak at m/z = 528, assigned as [Re(dmbpy)(CO)$_3$ + DMF], was detected by ESI-MS. The chloride ion is clearly removed during the ionization process, and the soft ionization of the CSI-MS enables detection of the Re complex as it is, without removal of the chloride ion. The peaks of the starting complex **1** decreased dramatically within 30 min of the photoirradiation, replaced by appearance of the peak assigned to the solvent-coordinated intermediate, [Re(dmbpy)(CO)$_3$DMF] (**2**, m/z = 528), which is formed by

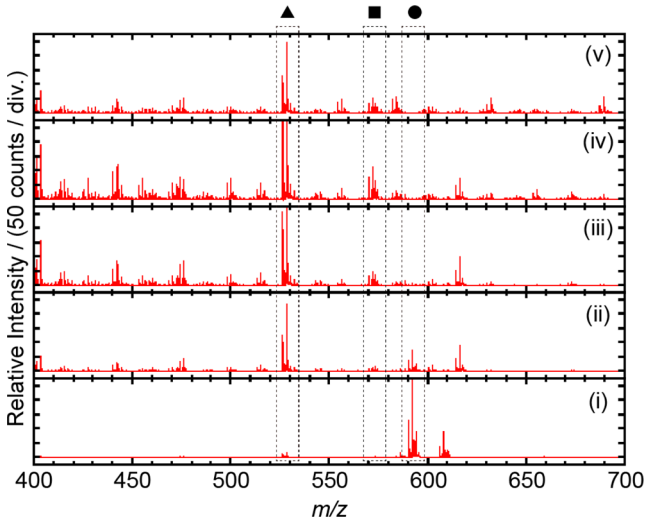

Figure 2. Positive-ion mode CSI-MS spectra of the reaction mixture upon (i) 0, (ii) 30, (iii) 180, (iv) 270, and (v) 1000 min of photoirradiation. The mass peak at m/z = 528 (▲) is assigned as the solvent-coordinated species, [Re(dmbpy)(CO)$_3$DMF] (**2**); m/z = 572 (■) as the CO_2 adduct, [Re(dmbpy)(CO)$_3$(CO_2) + DMF]; and m/z = 592 (●) as [Re(dmbpy)(CO)$_3$Cl + TEA + H].

dissociation of the Cl ligand after photoexcitation (Figure 2 (i), (ii)). The solvent-coordinated species **2** (m/z = 528) exhibited an interesting rise-and-decay profile during the photoirradiation (Figure 2 (iii)−(v); see also Figure 7b). The peak intensity gradually rose to a maximum around 270 min of photoirradiation. After 1000 min of photoirradiation, the intensity of the intermediate decreased gradually.

Among the signals observed in the positive-ion mode CSI-MS, the peaks at m/z = 403, 415, 427, 442, 455, 476, 500, 515, 528, 556, 570−574, and 616 might be derived from the Re−bipyridyl complexes including DMF or CO_2 as ligands, because the peak intensities also exhibited a rise-and-decay profile, being highest at the most reactive period. However, the peaks could not be characterized in sufficient detail, except those at m/z = 570−574, which will be analyzed in detail later. The other mass peaks with much smaller intensities, observed at m/z = 556, 584, and 604, showed a different time profile, with a monotonic increase throughout the photoirradiation. The corresponding species were clearly accumulating in the reaction mixture. Those peaks also were not able to be characterized well but might be ascribed to other Re complexes transformed from the starting complex **1** or decomposed as side products during the photoreaction. In summary, the observed mass peaks are classified into three groups: group I, which exhibited a monotonic decrease of their intensities (m/z = 592 and 608, assigned as the starting Re complex **1**); group II, which exhibited a rise-and-decay profile (m/z = 403, 415, 427, 442, 455, 476, 500, 515, **528** (assigned as solvent-coordinated species), **570−574** (assigned as CO_2-cooordinated species, as analyzed below), and 616); and group III, which exhibited a monotonic increase but with much smaller intensities (m/z = 556, 584, and 604) (Table S1).

Assignment of the Peaks at *m/z* = 570−574. Very interestingly, among the signals in group II, we have successfully observed the CO_2 adducts of the Re−bipyridyl complex as the key intermediates in the reaction mixture around m/z = 570−574 in the positive-ion mode CSI-MS. The observed peaks were carefully assigned as those of [Re-

dx.doi.org/10.1021/ja500403e | J. Am. Chem. Soc. 2014, 136, 6021−6030

(dmbpy)$(CO)_3CO_2$ + DMF] (**3**, m/z = 570, 572) and [Re(dmbpy)$(CO)_3CO_2H$ + DMF] (**3′**, m/z = 571, 573) (Figure S3). The isotope distribution caused by ^{185}Re (37.4%) and ^{187}Re (62.6%) afforded two main peaks for a compound containing one Re atom, with subpeaks due to natural-abundance ^{13}C in the ligands within the complex. The patterns around m/z = 570−574 showed four main peaks with subpeaks, indicating two species containing one Re atom in each being superimposed in this region, as shown in Figures 2 and 3

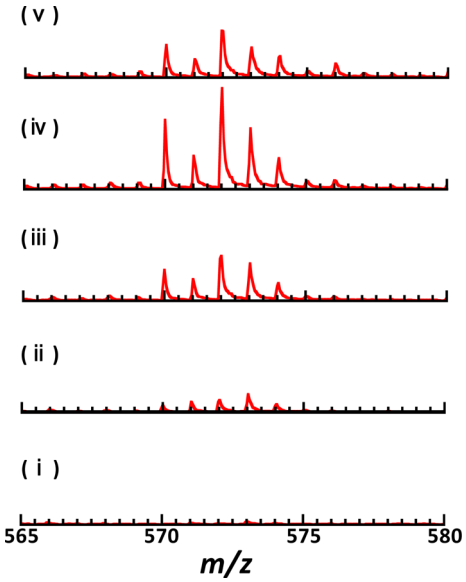

Figure 3. Comparison of the mass patterns assigned to a CO_2-coordinated intermediate at each photoirradiation time: (i) 0, (ii) 30, (iii) 180, (iv) 270, and (v) 1000 min.

without chlorine. It has been reported that the formate complex with oxygen atom coordination to Re, [Re(dmbpy)-$(CO)_3$(OCHO)] (**4**), was formed as a minor reaction product.[44−46] The formate complex **4** should have exactly the same mass number of m/z = 571, 573; thus, the observed peaks at m/z = 571, 573 may be ascribed to **4**. To check this possibility, we have synthesized the formate complex **4** according to the literature[37] and measured its CSI-MS signals (Figure S4). In fact, the mass pattern of **4** showed the peaks at m/z = 571, 573 with weak intensities, along with much more intense peaks, by a factor of ca. 7, at m/z = 600, 602. The intensity pattern, however, is very much different from that observed for the reaction mixture, where the peaks at m/z = 571, 573 had, in contrast, stronger intensity, by a factor of ca. 2, than those at m/z = 600, 602. Judging from the peak intensity at m/z = 600, 602 in the reaction mixture, the contribution of **4**, thus, should be smaller than 8% (1/2 × 1/7 = 1/14) compared to the peaks at m/z = 571, 573, even when **4** is involved in the reaction mixture. Moreover, the formate complex **4** had no peak at m/z = 570, whereas the reaction mixture definitely had peaks at m/z = 570, 572. These results strongly suggest that the peaks around m/z = 570−574 are derived mostly from a species different from **4**. Actually, when **4** was used as the starting photocatalyst for UV light irradiation, the quantum yield of CO evolution was very modest, only ∼2.1%, indicating that **4** should not be the active catalyst in the current system. Another probable candidate for the peaks at m/z = 571, 573 would be the Re−carboxylic acid complex, [Re(dmbpy)-$(CO)_3$(COOH)] (**5**). Here, we have also synthesized the Re^I−carboxylic acid complex **5** according to the literature.[47] When **5** was employed as the photocatalyst, the Φ_{CO} value was again observed to be very low, around 0.6%. This indicates that **5** is also not the active species that drives the photocatalytic reaction, though **5** was reported to form CO and bicarbonate Re complex in the dark.[48] The CSI-MS measurement of **5**, however, afforded a spectral pattern at m/z = 571, 573 fairly similar to that shown in Figure S4, while smaller peaks were observed at m/z = 570, 572 that are in different peak patterns from those of the reaction mixture. This indicates that the Re^I−carboxylic acid complex **5** may be involved in the reaction mixture and partly contributes to the spectra at m/z = 570−574, but another species, which shows stronger peaks at m/z = 570, 572, is definitely formed during photoreduction of CO_2 and is actually detected in the reaction mixture and assigned as the CO_2 adduct of the Re complex. It should be noted here that the details of the soft ionization in the chamber are not yet completely understood; in many cases, a molecule is observed as an ion, as it is, as an ion plus solvent, as a protonated form, and as a protonated form plus solvent, irrespective of the total charges on the original molecules in the positive-ion mode, as reported above in the case of the starting Re complex ([Re(dmbpy)$(CO)_3$Cl + TEA + H^+], m/z = 592).

The time course of the mass patterns assigned to the CO_2-coordinated intermediate of Re−bipyridyl complex (m/z = 570−574) upon photoirradiation is shown in Figure 3. After 30 min of photoirradiation (ii), the mass peaks at m/z = 570−574 appeared, where no peak was detected before the photoirradiation (i). The peak intensities at m/z = 570−574 also exhibited a rise-and-decay profile, without changing the peak patterns (Figure 3). These results strongly suggest that the signals at m/z = 570−574 are derived from the same species. As will be described later, the FTIR study clearly indicated the Re^{II}−COOH species, which was well correlated with the CSI-MS experiments. The species with peaks at m/z = 570−574 is thus assigned as [Re^{II}(dmbpy)$(CO)_3$COOH + DMF] (m/z = 571, 573) and its deprotonated form, [Re^{II}(dmbpy)-$(CO)_3(CO_2)$ + DMF] (m/z = 570, 572).

^{13}C Isotope Effect on the CSI Mass Spectra. To obtain a deeper insight into the spectral analysis of the CSI-MS experiment, a photochemical reaction of CO_2 reduction sensitized by [Re(dmbpy)$(CO)_3$Cl] (**1**) was carried out with isotope-labeled CO_2 ($^{13}CO_2$) under the same reaction conditions as above. The mass peaks of the reaction mixture with $^{13}CO_2$ were also detected in positive-ion mode CSI-MS. As a typical example, the mass spectra of the reaction mixture upon 180 min of photoirradiation in both $^{12}CO_2$ and $^{13}CO_2$ are compared in Figure 4. Very interestingly, among the group II

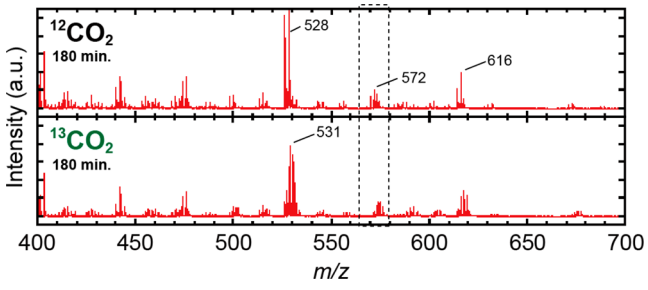

Figure 4. Positive-ion mode CSI-MS spectra of reaction mixtures under $^{12}CO_2$ and $^{13}CO_2$ atmosphere upon 180 min of photoirradiation, respectively.

dx.doi.org/10.1021/ja500403e | J. Am. Chem. Soc. 2014, 136, 6021−6030

mass peaks in the case of the $^{12}CO_2$ experiment, as classified above, which exhibited a rise-and-decay profile (m/z = 403, 415, 427, 443, 454, 476, 500, **528**, 556, **570**−**574**, 604, 616), only three peaks, m/z = 528 (solvent-coordinated species **2**), 570−574 (CO_2 adduct of Re complex, **3**/**3′**), and 616 (not well characterized), showed distinct shifts of their mass numbers, strongly suggesting that these are derived from the actual intermediates in the reaction pathway of CO_2 reduction photocatalyzed by the Re complex. Figure 5 shows how the

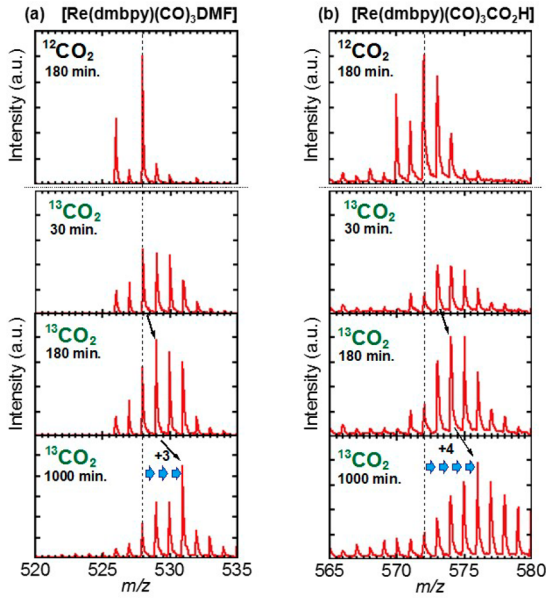

Figure 5. Mass pattern variation for (a) the DMF-coordinated and (b) $^{13}CO_2$-coordinated intermediates in the photochemical reaction cycle. The upper spectra are for $^{12}CO_2$, and the lower three are for $^{13}CO_2$. The arrows indicate the mass peak shifts upon photoirradiation.

mass peaks around m/z = 528 (solvent-coordinated species **2**) and 570−574 (CO_2 adduct of Re complex **3**/**3′**) change in the case of $^{13}CO_2$ when compared with those for $^{12}CO_2$.

As clearly seen in Figure 5, both peaks shifted to larger mass number, and the degree of the shifts became more pronounced during the photoirradiation. A careful inspection of Figure 5a indicates that, of the two main peaks (m/z = 526, 528), the intensity of the one at m/z = 526 gradually decreased and disappeared after 1000 min of photoirradiation, when the other strongest peak, m/z = 528, reached m/z = 531. This indicates that the solvent-coordinated Re complex clearly had an uptake of ^{13}C during the photoreaction, and the degree of ^{13}C uptake increased upon prolonged photoirradiation. The three mass unit shift (+3) of the main peak (from m/z = 528 to 531) indicates that three ^{13}C atoms were incorporated in the DMF-coordinated Re complex. This result coincides well with the previous NMR study, which showed that all three of the CO ligands of the Re complex were replaced with ^{13}CO during the photoreaction under $^{13}CO_2$ conditions.[8] The other peaks around m/z = 570−574 exhibited a more interesting feature: the most intense peak at m/z = 572 shifted to 576 after 1000 min photoirradiation (Figure 5b). The four mass unit shift (+4) clearly indicates an additional ^{13}C uptake, in addition to the ^{13}C uptake into the three CO ligands within the Re complex. This should be the most convincing evidence for the assignment of the peaks at m/z = 570−574 to the CO_2 adduct with the Re complex, since the uptake of four ^{13}C atoms can only be explained as further $^{13}CO_2$ incorporation as the sixth ligand to form the composition [Re(dmbpy)(^{13}CO)$_3$^{13}COOH + DMF]. Both peak shifts (from m/z = 572 to 576, and from m/z = 528 to 531) in the CSI-MS experiment proceeded gradually with photoirradiation, as seen in Figure 5, indicating that the peak shifts originate from a mixture of singly ^{13}C-incorporated species up to the fully incorporated species. Their compositions among the non-^{13}C-incorporated species and each ^{13}C species (one-^{13}C species, two-^{13}C species, three-^{13}C species for the DMF-coordinated Re complex, and one-^{13}C, two-^{13}C, three-^{13}C, four-^{13}C species for the CO_2 adduct of the Re complex) were carefully estimated by subtracting the contribution of each ^{13}C-incorporated species stepwise from the original spectra.

The detailed procedure for the analysis is described in the Supporting Information (Figure S5). The relative ratios among the ^{13}C species at each photoirradiation time are summarized in Figure 6. The incorporation of ^{13}C into the CO ligand indicates

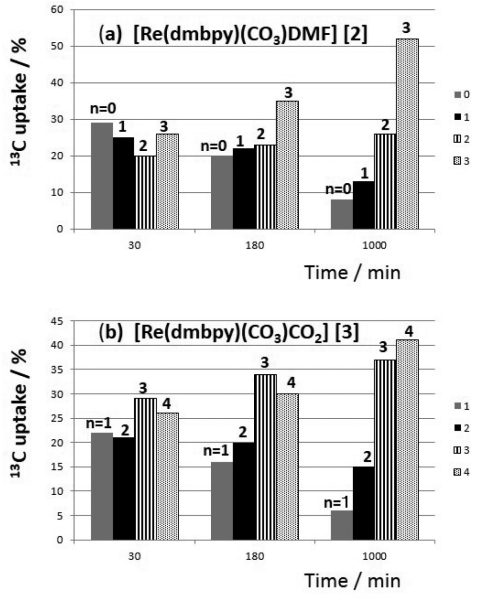

Figure 6. ^{13}C uptake into the key intermediates, (a) the DMF-coordinated Re complex **2** and (b) the CO_2 adduct of the Re complex **3**, upon photoirradiation. The turnover numbers are 1 (t = 30 min), 2.5 (t = 180 min), and 7 (t = 1000 min).

that the reduced product ^{13}CO generated from the CO_2 adduct of the Re complex replaces one of the three other CO ligands within the complex through axial−equatorial isomerization, or the ^{13}CO liberated into solution simply attacks the complex again to replace one of the three CO ligands. Since the solubility of CO in DMF is nearly negligible, this extremely low CO concentration may exclude the latter possibility.

An illustration of the ligand replacement with $^{13}CO_2$ in the CO_2 reduction cycle is shown in Scheme 2. In the CO_2 reduction cycle, a tetracarbonyl complex, **6**, would be transiently formed, although it was not detected by the CSI-MS experiment. One of the four CO ligands present just after the reaction of CO_2 reduction may be immediately eliminated from the Re complex, followed by axial−equatorial isomerization. The ^{13}C uptake distributions among the two intermediates, the DMF-coordinated species [Re(dmbpy)-(CO)$_3$DMF] (**2**) and the CO_2 adduct [Re(dmbpy)-(CO)$_3$(COO)] (**3**), provide very interesting mechanistic

dx.doi.org/10.1021/ja500403e | J. Am. Chem. Soc. 2014, 136, 6021−6030

Scheme 2. ^{13}C Uptake through Stepwise Replacement of CO Ligands of Re−Bipyridyl Complexes and Addition of CO_2 in the Photochemical Reduction Cycle

$[Re(dmbpy)(^{12}CO)_3DMF](n=0) \rightarrow$

$[Re(dmbpy)(^{12}CO)_3{}^{13}CO_2](n=1) \rightarrow$

$[Re(dmbpy)(^{12}CO)_2(^{13}CO)DMF](n=1) \rightarrow$

$[Re(dmbpy)(^{12}CO)_2(^{13}CO)^{13}CO_2](n=2) \rightarrow$

$[Re(dmbpy)(^{12}CO)(^{13}CO)_2DMF](n=2) \rightarrow$

$[Re(dmbpy)(^{12}CO)(^{13}CO)_2{}^{13}CO_2](n=3) \rightarrow$

$[Re(dmbpy)(^{13}CO)_3DMF](n=3) \rightarrow$

$[Re(dmbpy)(^{13}CO)_3{}^{13}CO_2](n=4)$

information. As shown in Figure 6, the relative distributions of ^{13}C uptakes of n = 1, 2, 3 in **2** are very similar to those of n = 2, 3, 4 for **3** at each time of photoirradiation, strongly suggesting that CO_2 simply adds to the DMF-coordinated complex **2** to form a species with an additional ^{13}C, the CO_2 adduct **3**. The DMF-coordinated Re complex **2** is thus supposed to be the actual precursor of the CO_2 adduct **3** in the reaction pathway, as discussed in the reaction mechanism shown below in Scheme 3. After CO_2 incorporation within the Re complex, the CO_2 adduct may have two options when it accepts the second electron to form CO: (1) replacing one of the tricarbonyls $(CO)_3$ within the Re complex to induce CO liberation from the tricarbonyl $(CO)_3$ or (2) escaping from the Re complex into solution, without the replacement as the evolving CO. In either case, CO is liberated into the gas phase over the reaction mixture, since the solubility of CO in DMF is nearly negligible. The former case induces ^{13}C uptake into the Re complex when $^{13}CO_2$ is used, while in the latter case the Re complex has no ^{13}C uptake, simply evolving CO. Among the data of Figure 6, those at 180 min photoirradiation, when the starting Re complex **1** has been nearly transformed into the DMF-coordinated species **2** and the CO_2 adduct **3**/**3**′, as can be observed in Figure 7, and the highest CO evolution was observed, were chosen for further analysis. The turnover number (TON) of CO formation means how many cycles of reaction each Re complex can drive. Thus, the relative ratio between the replacement of the tricarbonyls within the complex and the simple escape from the complex can be estimated from the TON and the non-^{13}C uptake distribution (n = 0) in Figure 6, as indicated in eq 1 and Scheme 2,, where α denotes the ratio

$$\alpha^{TON} = \text{ratio of non-}^{13}\text{C uptake species}(n = 0) \quad (1)$$

of the escaping versus the replacement of CO with tricarbonyls $(CO)_3$ in each CO formation. From the data, TON = 2.5, the relative percentage of the non-^{13}C uptake species for the DMF-coordinated complex **2** (0.20), the ratio α is calculated to be 0.53. A similar calculation for the one-^{13}C uptake species (n = 1) for the CO_2 adduct (0.16) yields α = 0.48. These results indicate that nearly half of the CO formed within the Re complex escapes from the complex, while the other half remains within the complex to replace the tricarbonyls $(CO)_3$. This is the first example to reveal the microscopic coordination chemistry of the Re complex, which provides an interesting deeper insight to understand the behavior.

Time Course of the Peak Intensity of Each Intermediate. As summarized above, the CSI-MS measurement of the reaction mixture afforded three kinds of peak signals. Group I exhibited a monotonic decay, and group II exhibited a rise and decay, while group III exhibited a monotonic increase with minor intensity. Since group III clearly is associated with side reactions such as decomposition of the Re complex on prolonged light irradiation, attention was focused on groups I and II, especially on the specific signal peaks, m/z = 592 (starting Re complex, $[Re(dmbpy)(CO)_3Cl]$, **1**) in group I, and m/z = 528 (solvent-coordinated Re complex, $[Re(dmbpy)(CO)_3DMF]$, **2**) and m/z = 570, 572 (CO_2 adduct of the Re complex $[Re(dmbpy)(CO)_3(CO_2)$ + DMF, **3**) in group II. The time course of the mass peaks m/z = 592, 528, and 572, which can be assigned as the key intermediates, is shown in Figure 7,

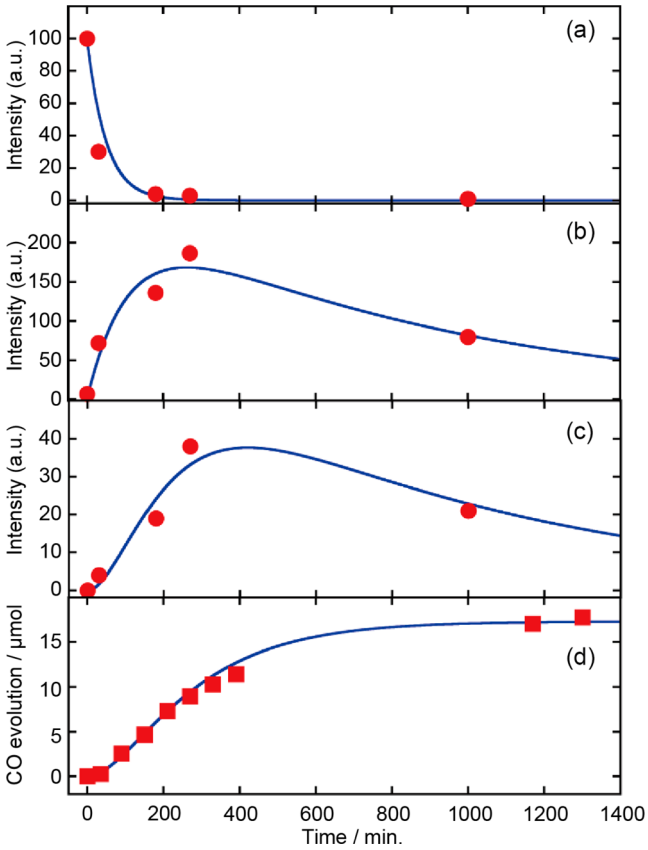

Figure 7. Time variations of the mass peaks, which can be assigned to the key species in the positive-ion mode CSI-MS and the resulting CO evolution: (a) m/z = 592 ($[Re(dmbpy)(CO)_3Cl + TEA + H^+]$) as **1**, (b) m/z = 528 ($[Re(dmbpy)(CO_3)DMF]$) as **2**, (c) m/z = 572 ($[Re(dmbpy)(CO_3)(CO_2)$ + DMF]) as **3**, and (d) the amount of CO evolution.

along with the CO evolution in the photoreaction. In Figure 7a, the intensity of the peak m/z = 592, assigned to the starting photocatalyst, **1**, decreased drastically within 180 min of photoirradiation, while the CO evolution reaction of CO_2 reduction maintained the reactivity (Figure 7d). This means that **1** is not the real active photocatalyst but forms an active catalyst in the reaction pathway. The DMF-coordinated intermediate **2** (m/z = 528) had appeared just after the photoirradiation in response to the decay of the starting Re complex, **1** (m/z = 592), as shown in Figure 7b. This corresponds to the dissociation of the Cl^- ligand from the Re−

dx.doi.org/10.1021/ja500403e | J. Am. Chem. Soc. 2014, 136, 6021−6030

bipyridyl complex by photoexcitation.[35,49] As regards the rapid decrease of **1** and the efficient production of **2**, Kutal et al. have reported that the strong reductant formed by deprotonation of the generated radical cation of triethanolamine ($[TEOA]^{\bullet+}$) by an electron transfer from TEOA to the excited Re complex might again reduce the original Re complex to induce an efficient removal of the halide ion followed by formation of the solvent-coordinated Re complex.[29] Under the current conditions of the photoreaction, it is similarly considered that the $[TEA]^{\bullet+}$ formed by an electron transfer from TEA to the excited Re complex would also afford a strong reductant by deprotonation to further reduce the Re complex **1** in the dark.

Interestingly, the time course of the peak intensity for the CO_2 adduct of the Re complex **3** (m/z = 572) shown in Figure 7c was different from that for the solvent-coordinated Re complex **2** in Figure 7b. The intensity for the CO_2 adduct of the Re complex **3** (m/z = 572, Figure 7c) increased in a delayed timing as compared with the solvent-coordinated species **2** (m/z = 528, Figure 7b) in the initial photoirradiation period. Careful inspection of the ratio of the peak intensity between the two signals at m/z = 528 (Figure 7b) and 572 (Figure 7c) at each time of observation clearly indicates that they exhibit different time profiles; the relative ratio of the intensity of (b) at m/z = 528 against that of (c) at m/z = 572 decreased systematically with the time of observation as 19 (t = 30 min), 8.6 (t = 180 min), 6.3 (t = 270 min), down to 3.9 (t = 1000 min). This indicates again that the species at m/z = 572 is not the CO_2-solvated one [Re(dmbpy)(CO_3)DMF + CO_2], but the CO_2-coordinated one [Re(dmbpy)(CO_3)(CO_2) + DMF]. If it were the CO_2-solvated species, it should exhibit exactly the same time profile as with [Re(dmbpy)(CO_3)DMF] (m/z = 528). The delayed timing may be reasonable, because the CO_2 adduct of the Re complex **3** would be formed through the reaction between the **2** and CO_2 in the reaction system.

More interestingly, the rise-and-decay profiles of the two intermediates, the solvent-coordinated species **2** and the CO_2 adduct of the Re complex **3**, correspond well to the CO evolution, as shown in Figure 7d; the time regions for the initial slow evolution, moderate stage, the most reactive stage, and decelerated stage correspond well to the time profile of each intermediate. This strongly suggests that the two species, the solvent-coordinated Re complex **2** and the CO_2 adduct **3**/**3′**, are the respective intermediates in the reaction pathway of photoreduction of CO_2 catalyzed by the Re complex. Since the current experiments were carried out under steady-state light irradiation conditions, the time profiles of each component and CO evolution only express qualitative features of the reaction. Even in this case, Figure 7 clearly indicates that the photoreaction should proceed through the following consecutive processes as **1** → **2** → [**3**/**3′**] → CO evolution.

FTIR Study of the Reaction Mixture during Photoirradiation. The CSI-MS results described above clearly indicate the detection of the key intermediate, the CO_2 adduct with the Re complex. The mass spectra, however, afford only information on the mass number, which is determined by the atomic composition. We were thus prompted to study further the FTIR spectra of the reaction mixture during the photoirradiation. The vibrational spectra should afford definite evidence of the nature of the bond. In the studies previously reported on IR measurements, the solvents employed were mostly CH_3CN or THF, due to their wide optical window for IR measurements. As described in the Introduction, however, CH_3CN and THF are both rather exceptional solvents, for which photoreduction of CO_2 has only poor reactivity, compared to a frequently used solvent such as DMF. Thus, we searched thoroughly for appropriate solvents that would allow both efficient CO_2 reduction and IR measurements, and we found that DMSO is a good candidate. The CO_2 photoreduction catalyzed by **1** proceeds with reactivity similar to that in DMF (Figure S6), and IR measurements are possible in the region down to 1500 cm^{-1} by choosing a proper optical path length within 0.2 mm. We have succeeded in obtaining an FTIR spectrum by means of a specially designed coaxial cylindrical IR cell with an Si window. During photoreduction of CO_2 under steady-state light irradiation, the FTIR signal was monitored by a rapid scan FTIR spectrometer under atmospheres of nitrogen, $^{12}CO_2$, and $^{13}CO_2$ (Figure 8). Very

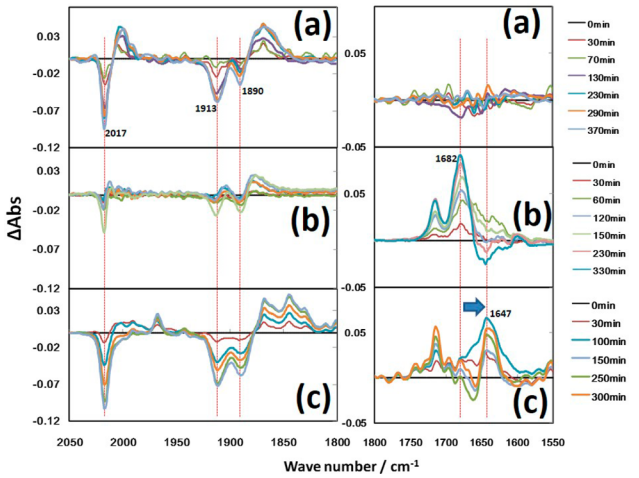

Figure 8. FTIR spectra of the reaction system of CO_2 reduction catalyzed by [Re(dmbpy)$(CO)_3$Cl] (**1**, 2 mM) in DMSO/TEA solvent (v/v = 15/1) under steady-state light irradiation: (a) under nitrogen atmosphere without CO_2, (b) under $^{12}CO_2$ atmosphere, and (c) under $^{13}CO_2$ atmosphere.

interestingly, the following distinct characteristic spectra were observed. Under nitrogen atmosphere in DMSO/TEA (15:1), we observed a clear depletion of the three carbonyl (CO triple bond) absorptions at 2017, 1910, and 1888 cm^{-1} of the starting Re complex **1** with appearance of the one-electron-reduced form of the Re complex around 2000 and 1870 cm^{-1} (Figure 8a). In the 1600−1700 cm^{-1} region, however, almost no signal was observed under nitrogen atmosphere (Figure 8a). Under $^{12}CO_2$ atmosphere, on the other hand, a clear signal appeared at 1682 cm^{-1} along with those of the one-electron-reduced form of the Re complex (Figure 8b). This band clearly shifted to a smaller wavenumber (1647 cm^{-1}) under $^{13}CO_2$ (Figure 8c), and the peaks of the one-electron-reduced form also exhibited substantial shifts and became broader. These results clearly indicate that the 1682 cm^{-1} band (Figure 8b) is due to the introduction of CO_2 and should be ascribed to the key intermediate in the reaction pathway of the photoreduction catalyzed by the Re complex. The spectral broadening of the CO region under $^{13}CO_2$ is well correlated with the ^{13}C uptake into CO ligands during the photoreaction (Figure 6). The wavenumber 1682 cm^{-1} corresponds exactly to the region for the C═O vibration. Comparisons with the synthesized formate complex, Re^{I}−OCHO (**4**, 2016, 1908, 1886, 1625 cm^{-1}), the carboxylic acid, Re^{I}−COOH (**5**, 2003, 1890, 1605 cm^{-1}) in DMSO/TEA (15:1), and DFT calculations have led to the

dx.doi.org/10.1021/ja500403e | J. Am. Chem. Soc. 2014, 136, 6021−6030

conclusion that the transient species is definitely different from **4**/**5** and is assigned as Re^{II}–COOH, which could be formed through the electrophilic attack of CO_2 against the one-electron-reduced form of the Re complex. This process should be a two-electron oxidative addition for the Re atom; that is, the Re^0 species (one-electron-reduced form of the Re^I complex) would be converted to a Re^{II} species upon addition of CO_2. The second electron transfer, from either the one-electron-reduced form of the Re complex accumulated within the system or a carbon radical possibly formed through the deprotonation of $[TEA]^{\bullet+}$, would evolve CO and regenerate the solvent-coordinated Re^I species **2**. It should be noted here that CSI-MS experiment in DMF/TEA (v/v = 5/1) exhibited both the deprotonated form of the CO_2 adduct, $[Re^{II}(dmbpy)(CO)_3(CO_2)]$ (**3**, m/z = 570, 572), and the protonated form, $[Re^{II}(dmbpy)(CO)_3COOH]$ (**3′**, m/z = 571, 573), while only the protonated form, **3′** (1682 cm^{-1}), was detected by FTIR measurement in DMSO/TEA (15/1). The difference might be caused by the characteristic soft ionization in the CSI-MS chamber, the different concentration of the base TEA in DMF and DMSO, or the nature of the solvents themselves.

Reaction Mechanism of the Photoreduction Catalyzed by the Re Complex. These observations are well correlated with the previous speculation on the reaction mechanism of photoreduction of CO_2 catalyzed by the Re complex shown in Scheme 1, leading to a deeper insight. The direct detection of the two key intermediates, **2** and **3**/**3′**, in this study definitely enables us to depict the reaction mechanism in a more detailed manner in Scheme 3.

Scheme 3. Photochemical CO_2 Reduction Cycle Sensitized by $[Re(dmbpy)(CO)_3Cl]$ (1)

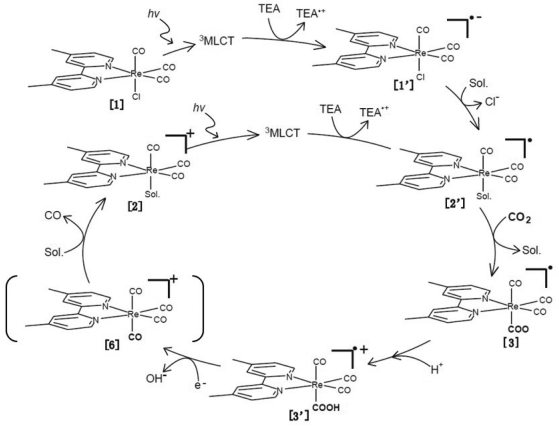

The primary reaction cycles under steady-state light irradiation proceed as follows:

(1) The starting Re complex **1** undergoes one-electron reduction by a reductive quenching of the excited Re complex **1** in its ^{3}MLCT state by TEA to form the radical anion of **1** (**1′** in Scheme 3).

(2) Chloride ion is subsequently eliminated, along with replacement with the solvent DMF to form the one-electron-reduced form of the solvent-coordinated Re complex, **2′**.

(3) The one-electron-reduced form of the solvent-coordinated Re complex, **2′**, undergoes an electrophilic attack by CO_2 along with protonation to form the CO_2 adduct of the Re complex, **3′**.

(4) The CO_2 adduct of the Re complex, **3′**, accepts another electron, probably from the one-electron-reduced form of the starting Re complex **1′**, the one-electron-reduced form of the solvent-coordinated Re complex **2′**, or a carbon radical possibly formed through the deprotonation of $[TEA]^{\bullet+}$ to evolve CO, along with the regeneration of the solvent-coordinated Re complex **2**.

(5) The solvent-coordinated Re complex **2** absorbs UV light to form the one-electron-reduced solvent-coordinated Re complex, **2′**, driving the continuous reaction cycle.

The DMF-coordinated Re complex **2**, thus, would be the major species for the light absorption to drive the reaction after the induction period of 30 min.

One of the most curious subjects to be clarified in the CO_2 photoreduction is the nature of the electron donor for the second electron, which reduces the CO_2 adduct of the Re complex ($[Re^{II}(dmbpy)(CO)_3COOH]$ (**3′**). In the CSI-MS and FTIR studies, there was no indication of a Re complex dimer formation, which was postulated by Fujita et al.[27,35] Recently, the Kubiak group reported formation of Re^I–COOH, the synthesis and chemical behavior of which had been studied by Gibson,[47] in an electrochemical simultaneous two-electron reduction process of the Re–bipyridyl complex.[50] This is also negative evidence for the dimer mechanism. In the photochemical system, the total two-electron reduction of CO_2 to form CO is proceeding in a stepwise manner, as described above. The second electron, thus, should come from either a carbon radical possibly formed through the deprotonation of $[TEA]^{\bullet+}$ or a one-electron-reduced Re complex species such as **2′**. The highly efficient CO_2 reduction reported by the Ishitani group may be due to the relatively long lifetime of the one-electron species for $[Re(dmbpy)(CO)_3\{P(OEt)_3\}]$.[11] Eventually, the photocatalytic cycle will be maintained until the Re–bipyridyl complex is decomposed through side reactions during prolonged photoirradiation. The FTIR study has afforded clear, conclusive information about the assignment of the CO_2 adduct of the Re complex, **3**/**3′**, observed in the CSI-MS. The observed species at m/z = 571, 573 is not a simple CO_2-solvated one such as $[Re(dmbpy)(CO)_3DMF + CO_2 + H^+]$ or $[Re(dmbpy)(CO)_3 + DMF + CO_2 + H^+]$ but the chemical-bonded CO_2 adduct, $[Re(dmbpy)(CO)_3COOH + DMF]$.

■ CONCLUSIONS

By means of sophisticated CSI-MS measurements of the reaction mixture, we have successfully detected the DMF-coordinated Re complex $[Re(dmbpy)(CO)_3DMF]$ (**2**) as the light-absorbing species to drive photoreduction of CO_2. The key intermediate, the CO_2-coordinated Re–bipyridyl complex, $[Re(dmbpy)(CO)_3COOH]$ (**3**), was also successfully detected for the first time by CSI-MS. The mass spectra for the reaction mixture with the isotopically labeled $^{13}CO_2$ provided clear evidence for the incorporation of CO_2 into the Re–bipyridyl complex. It was revealed that the starting chloride complex, $[Re(dmbpy)(CO)_3Cl]$ (**1**), was rapidly transformed into the DMF-coordinated Re complex through the initial cycle of the photoreduction of CO_2. The observed induction period in the time profile of the CSI-MS signals can well explain the subsequent formation of the CO_2-coordinated intermediate **3** from the DMF-coordinated Re–bipyridyl complex **2**. FTIR spectra in DMSO clearly indicated that the CO_2-coordinated intermediate should be the Re^{II}–COOH complex. Thus, a detailed understanding of the mechanism of photochemical

dx.doi.org/10.1021/ja500403e | J. Am. Chem. Soc. 2014, 136, 6021–6030

CO_2 reduction sensitized by the Re−bipyridyl complex as a benchmark reaction has now been obtained.

■ ASSOCIATED CONTENT

Supporting Information

Mass pattern for [Re(dmbpy)$(CO)_3$Cl + TEA + H] in the positive-ion mode CSI-MS; mass spectrum for **1** in the ordinary ESI-MS; mass pattern analysis for **3** (m/z = 570, 572) and **3′** (m/z = 571, 573); CSI-MS spectra for alternatively synthesized **4** and **5**; analysis of ^{13}C uptake into **2**; CO evolution catalyzed by **1** in DMSO/TEA solvent (v/v = 15/1); FTIR spectra of **4** and **5**; and characteristic peaks observed in the positive-ion mode CSI-MS spectra of the reaction mixture. This material is available free of charge via the Internet at http://pubs.acs.org.

■ AUTHOR INFORMATION

Corresponding Author

inoue-haruo@tmu.ac.jp

Present Address

[§]School of Medicine, Tokyo Medical University, 6-1-1 Shinjuku, Shinjuku-ku, Tokyo 160-8402, Japan

Notes

The authors declare no competing financial interest.

■ ACKNOWLEDGMENTS

This work was partially supported by a Grant-in-Aid for Scientific Research on Innovative Areas from the Ministry of Education, Culture, Sports, Science and Technology of Japan. The authors thank Dr. Tsuyoshi Tsuchibuchi at Shimadzu Corp. for kind help with the FTIR measurements.

■ REFERENCES

(1) Morris, A. J.; Meyer, G. J.; Fujita, E. *Acc. Chem. Res.* **2009**, *42*, 1983.

(2) Inoue, H.; Shimada, T.; Kou, Y.; Nabetani, Y.; Masui, D.; Takagi, S.; Tachibana, H. *ChemSusChem* **2011**, *4*, 173.

(3) (a) Halmann, M. *Nature* **1978**, *275*, 115. (b) Ito, K.; Ikeda, S.; Yoshida, M.; Ohta, S.; Iida, T. *Bull. Chem. Soc. Jpn.* **1984**, *57*, 583. (c) Taniguchi, I.; Aurian-Blajeni, B.; Bockris, J. O'. M. *Electrochim. Acta* **1984**, *29*, 923. (d) Taniguchi, I.; Aurian-Blajeni, B.; Bockris, J. O'. M. *J. Electroanal. Chem.* **1984**, *161*, 385. (e) Yoneyama, H.; Sugimura, K.; Kuwabata, S. *J. Electroanal. Chem.* **1988**, *249*, 143. (f) Bockris, J. O'. M.; Wass, J. C. *J. Electrochem. Soc.* **1989**, *136*, 2521. (g) Ueda, J.; Nakabayashi, S.; Ushizaki, J.; Uosaki, K. *Chem. Lett.* **1993**, 1747. (h) Flaisher, H.; Tenne, R.; Halmann, M. *J. Electroanal. Chem.* **1996**, *402*, 97. (i) Bradley, M. G.; Tysak, T.; Graves, D. J.; Viachopoulos, N. A. *J. Chem. Soc., Chem. Commun.* **1983**, 349. (j) Cabrera, C. R.; Abruna, H. D. *J. Electroanal. Chem.* **1986**, *209*, 101. (k) Liu, J. F.; ChunYu, B. Z. *J. Electroanal. Chem.* **1992**, *324*, 191. (l) Hinogami, R.; Nakamura, Y.; Yae, S.; Nakato, Y. *J. Phys. Chem.* **1998**, *102*, 974. (m) Aurian-Blajeni, B.; Halmann, M.; Manassen, J. *Sol. Energy Mater.* **1983**, *8*, 425. (n) Sears, W. M.; Morrison, S. R. *J. Phys. Chem.* **1985**, *89*, 3295. (o) Parkinson, B. A.; Weaver, P. F. *Nature* **1984**, *309*, 148. (p) Canfield, D.; Frese, K. W., Jr. *J. Electrochem. Soc.* **1983**, *130*, 1772. (q) Noda, H.; Ikeda, S.; Saito, Y.; Nakamura, T.; Maeda, M.; Ito, K. *Denki Kagaku* **1989**, *57*, 1117. (r) Hashimoto, K.; Fujishima, A. In *Carbon Dioxide Chemistry: Environmental Issues*; Pradier, J. P., Pradier, C. M., Eds.; The Royal Institute of Technology: Stockholm, 1994; pp 388. (s) Hirota, K.; Tryk, D. A.; Yamamoto, T.; Hashimoto, K.; Okawa, M.; Fujishima, A. *J. Phys. Chem. B* **1998**, *102*, 9834.

(4) (a) Seshadri, G.; Lin, C.; Bocarsly, A. B. *J. Electroanal. Chem.* **1994**, *372*, 145. (b) Barton, C. E.; Lakkaraju, P. S.; Rampulla, D. M.; Morris, A. J.; Abelev, E.; Bocarsly, A. B. *J. Am. Chem. Soc.* **2010**, *132*, 11539. (c) Morris, A. J.; McGibbon, R. T.; Bocarsly, A. B. *ChemSusChem* **2011**, *4*, 191. (d) Barton, E. E.; Rampulla, D. M.; Bocarsly, A. B. *J. Am. Chem. Soc.* **2008**, *130*, 6342.

(5) Keith, J. A.; Carter, E. A. *J. Am. Chem. Soc.* **2012**, *134*, 7580.

(6) Iizuka, K.; Wato, T.; Miseki, Y.; Saito, K.; Kudo, A. *J. Am. Chem. Soc.* **2011**, *133*, 20863.

(7) Hawecker, J.; Lehn, J.-M.; Ziessel, R. *J. Chem. Soc., Chem. Commun.* **1983**, *0*, 536.

(8) Hawecker, J.; Lehn, J.-M.; Ziessel, R. *Helv. Chim. Acta* **1986**, *69*, 1990.

(9) Kou, Y.; Nakatani, S.; Sunagawa, G.; Tachikawa, Y.; Masui, D.; Shimada, T.; Takagi, S.; Tryk, D. A.; Nabetani, Y.; Tachibana, H.; Inoue, H. *J. Catal.* **2014**, *310*, 57.

(10) Hori, H.; Johnson, F. P. A.; Koike, K.; Ishitani, O.; Ibusuki, T. *J. Photochem. Photobiol. A: Chemistry* **1996**, *96*, 171.

(11) Takeda, H.; Koike, K.; Inoue, H.; Ishitani, O. *J. Am. Chem. Soc.* **2008**, *130*, 2023.

(12) Gholamkhass, B.; Mametsuka, H.; Koike, K.; Tanabe, T.; Furue, M.; Ishitani, O. *Inorg. Chem.* **2005**, *44*, 2326.

(13) Sato, S.; Koike, K.; Inoue, H.; Ishitani, O. *Photochem. Photobiol. Sci.* **2007**, *6*, 454.

(14) Bian, Z.-Y.; Sumi, K.; Furue, M.; Sato, S.; Koike, K.; Ishitani, O. *Inorg. Chem.* **2008**, *47*, 10801.

(15) Gabrielsson, A.; Lindsay Smith, J. R.; Perutz, R. N. *Dalton Trans.* **2008**, 4259.

(16) Koike, K.; Naito, S.; Sato, S.; Tamaki, Y.; Ishitani, O. *J. Photochem. Photobiol. A: Chemistry* **2009**, *207*, 109.

(17) Kiyosawa, K.; Shiraishi, N.; Shimada, T.; Masui, D.; Tachibana, H.; Takagi, S.; Ishitani, O.; Tryk, D. A.; Inoue, H. *J. Phys. Chem. C* **2009**, *113*, 11667.

(18) Schneider, J.; Vuong, K. Q.; Calladine, J. A.; Sun, X.-Z.; Whitwood, A. C.; George, M. W.; Perutz, R. N. *Inorg. Chem.* **2011**, *50*, 11877.

(19) Sato, S.; Morikawa, T.; Kajino, T.; Ishitani, O. *Angew. Chem.* **2013**, *125*, 1022.

(20) (a) Sato, S.; Morikawa, T.; Saeki, S.; Kajino, T.; Motohiro, T. *Angew. Chem., Int. Ed.* **2010**, *49*, 5101. (b) Suzuki, T. M.; Tanaka, H.; Morikawa, T.; Iwaki, M.; Sato, S.; Saeki, S.; Inoue, M.; Kajino, T.; Motohiro, T. *Chem. Commun.* **2011**, *47*, 8673.

(21) Arai, T.; Sato, S.; Uemura, K.; Morikawa, T.; Kajino, T.; Motohiro, T. *Chem. Commun.* **2010**, *46*, 6944.

(22) Arai, T.; Tajima, S.; Sato, S.; Uemura, K.; Morikawa, T.; Kajino, T. *Chem. Commnun.* **2011**, *47*, 12664.

(23) Sato, S.; Arai, T.; Morikawa, T.; Uemura, K.; Suzuki, T. M.; Tanaka, H.; Kajino, T. *J. Am. Chem. Soc.* **2011**, *133*, 15240.

(24) Takeda, H.; Ishitani, O. *Coord. Chem. Rev.* **2010**, *254*, 346.

(25) Doherty, M. D.; Grills, D. C.; Muckerman, J. T.; Polyansky, D. E.; Fujita, E. *Coord. Chem. Rev.* **2010**, *254*, 2472.

(26) Windle, C. D.; Perutz, R. N. *Coord. Chem. Rev.* **2012**, *256*, 2562.

(27) Agarwal, J.; Fujita, E.; Schaefer, H. F.; Muckerman, J. T. *J. Am. Chem. Soc.* **2012**, *134*, 5180.

(28) Schneider, J.; Jia, H.; Muckerman, J. T.; Fujita, E. *Chem. Soc. Rev.* **2012**, *41*, 2036.

(29) Kutal, C.; Weber, M. A.; Ferraudi, G.; Geiger, D. *Organometallics* **1985**, *4*, 2161.

(30) Kutal, C.; Corbin, A. J.; Ferraudi, G. *Organometallics* **1987**, *6*, 553.

(31) Kalyanasundaram, K. *J. Chem. Soc., Faraday Trans. 2* **1986**, *82*, 2401.

(32) Hori, H.; Koike, K.; Suzuki, Y.; Ishizuka, M.; Tanaka, J.; Takeuchi, K.; Sasaki, Y. *J. Mol. Catal. A: Chemical* **2002**, *179*, 1.

(33) Hori, H.; Ishihara, J.; Koike, K.; Takeuchi, K.; Ibusuki, T.; Ishitani, O. *Chem. Lett.* **1997**, *26*, 273.

(34) Hori, H.; Ishihara, J.; Koike, K.; Takeuchi, K.; Ibusuki, T.; Ishitani, O. *J. Photochem. Photobiol. A: Chemistry* **1999**, *120*, 119.

(35) Hayashi, Y.; Kita, S.; Brunschwig, B. S.; Fujita, E. *J. Am. Chem. Soc.* **2003**, *125*, 11976.

(36) Shinozaki, K.; Hayashi, Y.; Brunschwig, B.; Fujita, E. *Res. Chem. Intermed.* **2007**, *33*, 27.

(37) Johnson, F. P. A.; George, M. W.; Hartl, F.; Turner, J. J. *Organometallics* **1996**, *15*, 3374.
(38) Scheiring, T.; Klein, A.; Kaim, W. *J. Chem. Soc., Perkin Trans. 2* **1997**, 2569.
(39) Klein, A.; Vogler, C.; Kaim, W. *Organometallics* **1996**, *15*, 236.
(40) Kunimura, M.; Sakamoto, S.; Yamaguchi, K. *Org. Lett.* **2002**, *4*, 347.
(41) Yamaguchi, K. *J. Mass Spectrom.* **2003**, *38*, 473.
(42) Worl, L. A.; Duesing, R.; Chen, P.; Ciana, L. D.; Meyer, T. J. *J. Chem. Soc., Dalton Trans.* **1991**, *11*, 849.
(43) Bruckmeier, C.; Lehenmeier, M. W.; Reithmeier, R.; Rieger, B.; Herranz, J.; Kavakli, C. *Dalton Trans.* **2012**, *41*, 5026.
(44) Sullivan, B. P.; Meyer, T. J. *J. Chem. Soc., Chem. Commnun.* **1984**, 1244.
(45) Gibson, D. H.; He, H. *Chem. Commnun.* **2001**, 2082.
(46) Hori, H.; Takano, Y.; Koike, K.; Sasaki, Y. *Inorg. Chem. Commun.* **2003**, *6*, 300.
(47) (a) Gibson, D. H.; Yin, X. *J. Am. Chem. Soc.* **1998**, *120*, 11200. (b) Gibson, D. H.; Yin, X.; He, H.; Mashuta, M. S. *Organometallics* **2003**, *22*, 337.
(48) Hori, H.; Johnson, F. P. A.; Koike, K.; Takeuchi, K.; Ibusuki, T.; Ishitani, O. *J. Chem. Soc., Dalton Trans.* **1997**, 1019.
(49) Agarwal, J.; Sanders, B. C.; Fujita, E.; Schaefer, H. F., III; Harrop, T. C.; Muckerman, J. T. *Chem. Commun.* **2012**, *48*, 6797.
(50) Sampaon, M. D.; Froelich, J. D.; Smieja, J. M.; Benson, E. E.; Sharp, I. D.; Kubiak, C. P. *Energy Environ. Sci.* **2013**, *6*, 3748.